Journal of Applied Pharmaceutical Science Vol. 12(04), pp 159-169, April, 2022
Available online at http://www.japsonline.com
DOI: 10.7324/JAPS.2022.120418
ISSN 2231-3354

ADME studies of TUG-770 (a GPR-40 inhibitor agonist) for the treatment of type 2 diabetes using SwissADME predictor: *In silico* study

Khaldun M. Al Azzam[1*], El-Sayed Negim[2], Hassan Y. Aboul-Enein[3]

[1]Department of Pharmaceutical Sciences, Pharmacological and Diagnostic Research Center (PDRC), Faculty of Pharmacy, Al-Ahliyya Amman University, Amman, Jordan.
[2]Laboratory of Advanced Materials and Technology, Kazakh-British Technical University, Tole bi St. 59, Almaty, Kazakhstan.
[3]Department of Pharmaceutical and Medicinal Chemistry, Pharmaceutical and Drug Industries Research Division, National Research Center, Giza, Egypt.

ARTICLE INFO

Received on: 11/12/2021
Accepted on: 05/02/2022
Available Online: 05/04/2022

Key words:
SwissADME, TUG-770, ChemDraw, *in silico* prediction.

ABSTRACT

In vivo absorption, delivery, metabolism, and elimination (ADME) testing is considered expensive, time-consuming, and animal lives put at risk, while *in silico* ADME testing is safer, easier, and faster. The aim of this study is to predict the ADME profile of drug candidates prior to their synthesis. TUG-770 *in silico* ADME experiments will be predicted in this study to tell what to expect from the clinical trials, to find a link between *in vivo* and *in silico* findings, and to improve the structure of TUG-770 so that biological activity is not harmed (unaffected) while unwanted ADME effects are reduced. The 2D and 3D structures of TUG-770 were drawn using ChemDraw 3D-Ultra version 19.0.0.22 by minimizing the energy using MM2 and Molecular Orbital Package (MOPAC) with the minimum Root-Mean-Square (RMS) gradient set to 0.01. The bioavailability radar revealed that the colored areas were bioavailable, which have properties like lipophilicity, flexibility, saturation scale, and polarity, which are the most favorable physicochemical environments for oral bioavailability and solubility. The molecular formula of the molecule, according to its physicochemical properties, is $C_{19}H_{14}FNO_2$ [307.32 (g/mol)]. This compound has 23 heavy atoms and 12 aromatic heavy atoms. In the sp^3 hybridization, 0.16% of carbon atoms are active.

INTRODUCTION

Drug research entails determining the safety and toxicity of potential new drugs, as well as developing a target receptor hypothesis for a specific condition and screening the new drug candidates' *in vitro* and/or *in vivo* biological activities. Conducting drug metabolism and pharmacokinetics tests, also known as ADMET, which means absorption, delivery, metabolism, elimination, and toxicity experiments, is an important part of drug discovery (Guoli *et al*., 2021; Leonardo and Adriano, 2019; Longfei *et al*., 2019; Yuhua *et al*., 2019). The use of early absorption, delivery, metabolism, and excretion (ADME) assessment has significantly reduced the number of compounds that fail clinical trials (Akbar *et al*., 2017; Kaitin, 2008; Mishra and Dahima, 2019).

Preclinical ADME's main goal is to remove poor drug candidates early in the drug development process, allowing resources to be spent on promising candidates (Mishra and Dahima, 2019). Since the 1950s, regulatory agencies have focused on *in vivo* research to predict how new molecules would behave in the body of humans (Arora *et al*., 2008). Bioavailability, pharmacokinetics, metabolism, tissue distribution, and toxicity are usually evaluated in one non-rodent and one rodent species preceding administering a medication to a person in a clinical trial (dog or nonhuman primate) in phase 1. Radioactively labeled compounds are commonly used in the appropriate technique for biodistribution assessment. Animal studies and synthesizing enough radioactively labeled compounds both take time and resources (Oldendorf, 1970).

**Corresponding Author*
Khaldun M. Al Azzam, Department of Pharmaceutical Sciences, Pharmacological and Diagnostic Research Center (PDRC), Faculty of Pharmacy, Al-Ahliyya Amman University, Amman, Jordan.
E-mail: azzamkha @ yahoo.com

As a result, these assays are used later in the preclinical research process, when there are more tools available to study the few molecules that have made it that far. Thanks to advancements in cell and molecular biology, high-throughput sampling, and miniaturization technology in the 1990s, as well as stem cell-derived models at the turn of the century, early *in silico* ADME experiments have been developed to predict *in vivo* animal and human outcomes at a pace and cost-effectiveness suitable for the early discovery period (Mishra and Dahima, 2019; Oldendorf, 1970).

Preclinical drug testing necessitates the use of animals, which is time-consuming and expensive, as well as potentially causes individual pain. This has compelled scientists to look for ways to cut down on not just the time expended on drug detection experiments, but also the number of animals involved and their care by humans. To achieve this end, several new *in silico* techniques known as "alternatives" or "substitutes" for animal use in drug research have been developed (Arora *et al*., 2008).

The benefits of these choices involve a reduction in the number of animals utilized, the capability to deliver results rapidly, cost savings, and the versatility to monitor the experiment's variables (Mishra and Dahima, 2019). The advancement of ADME profiling has reduced the number of drug candidates failing in clinical trials due to ADME issues, while also providing critical early information for drug candidate safety and toxicity prediction.

The SwissADME web tool is a free piece of software that predicts the following: physicochemical properties, distribution, metabolism, elimination, absorption, and also pharmacokinetic properties of molecules under investigation, all of which are important steps in the process of moving forward with clinical trials (Mishra and Dahima, 2019; Yusuf *et al*., 2020). Lipophilicity, flexibility, saturation, polarity, size, and solubility are among the six most significant physicochemical properties considered (Pires *et al*., 2018).

Parameters in druglikeliness can be investigated using a collection of rules developed by different pharmaceutical companies, which establish the correlation between biological activities and properties of pharmacokinetic, and that must be followed for *in vivo* action (Cheng *et al*., 2012). For instance, Pfizer established the Lipinski rule of five which states that the molecule's molecular weight should be less than 500 Da, also the H-bond acceptor is less than 10, the H-bond donor should be higher than 5, the logP value should be less than 5, and biological transporters should be avoided (Mishra and Dahima, 2019).

The logP value must range from −0.4 to +5.6; the molar refractivity must be between 40 and 130; the molecular weight must be within the range of 180–480; and the number of the atoms must be between 20 and 70, including hydrogen bond donor and acceptor, according to Amgen's Ghose rule (Cheng *et al*., 2012). The Egan rule notes that the logP value and topological polar surface area (TPSA) should not exceed 5.88 and 131.6, respectively, for predicting human intestinal absorption (Mishra and Dahima, 2019).

Based on small molecule lipophilicity and polarity computations, the BOILED-egg model is proposed as an efficient predictive model. The permeability glycoprotein (P-gp) substrate is used to measure active efflux across biological membranes. It defends the Central Nervous System (CNS) from xenobiotics and is overexpressed in tumor cells. Five main isoforms, namely CYP1A2, CYP2C19, CYP2C9, CYP2D6, and CYP3A4, are substrates for 50%–90% of molecules. Inhibition of these isoenzymes is likely to be one of the more frequent sources of pharmacokinetics-related drug–drug interactions and can result in toxic ADME due to drug/metabolite accumulation (Potts and Guy, 1992).

TUG-770, 3-(4-((2-(cyanomethyl)phenyl)ethynyl)-2-fluorophenyl)propanoic acid, is a GPR-40 inhibitor in clinical trials (Fig. 1). This study aims to predict the *in silico* ADME experiments of TUG-770, to understand the predictable outcome of clinical trials, to find a link between *in vivo* and *in silico* outcomes, and to enhance TUG-770's structure such that biological activity is not harmed while unwanted ADME effects are decreased. To our

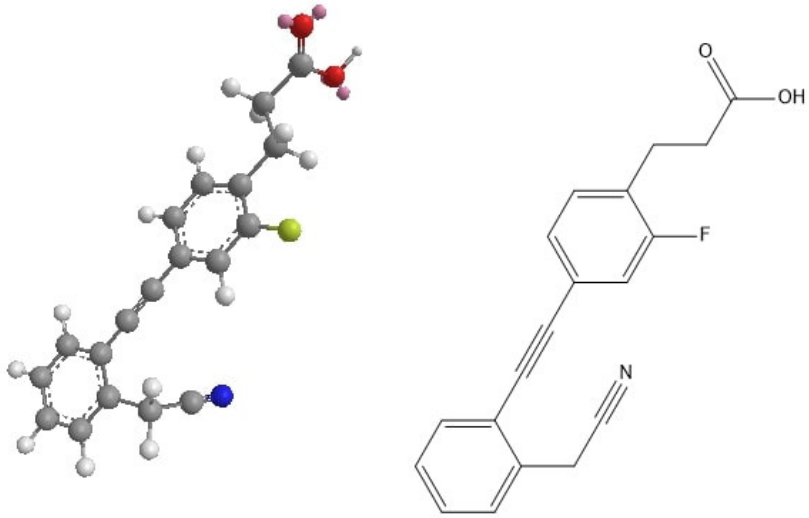

Figure 1. Chemical structure of TUG-770.

knowledge, this is the first research using SwissADME predictor to conduct *in silico* ADME studies of TUG-770 for the treatment of type 2 diabetes.

MATERIALS AND METHODS

SwissADME is a free online platform for determining the drug-likeness, pharmacokinetics, and medicinal chemistry related to the stability of small molecules (Noemi *et al*., 2020; Tianshu *et al*., 2021). In comparison to the state-of-the-art of ADME (free web-based tools) and pharmacokinetics, such as pk-CSM (Pires *et al*., 2018) and admetSAR (Cheng *et al*., 2012), and aside from unique access to proficient methods, such as ilogP (Daina *et al*., 2014) or the BOILED-egg (Daina and Zoete, 2016), strong points of SwissADME include input methods diverse, computation for various molecules, and the ability to display, save, and exchange results (per-molecule basis) or via global, and interactive graphs. SwissADME is considered now part of the SwissDrugDesign workspace (Daina *et al*., 2014; Daina and Zoete, 2017).

ChemDraw was used to draw the 2D structure of TUG-770, and ChemDraw 3D-Ultra version 19.0.0.22 was used to draw the 2D and 3D structures by minimizing energy with MM2 and MOPAC, with the minimum RMS gradient set to 0.01. The structure smiley was introduced after the structure was imported. The results of the SwissADME drug design study have been recorded.

RESULTS AND DISCUSSION

According to Verber, a GlaxoSmithKline (GSK) pharmaceuticals spokesperson, some drugs, such as steroids, should have a molecular weight of more than 500 Da, 10 or even lower rotatable bonds, and a polar surface area of lower than 140 A^o. The Muegge rule, proposed by Bayer Pharmaceuticals, defined the following parameters: number of rings (> 7), number of carbon atoms (< 4), number of heteroatoms (> 1), number of rotatable bonds (< 15), hydrogen bond donor atoms (< 5), and hydrogen bond acceptor (> 10). Molecular weight ranged from 200 to 600 D; logP was between the range −2 and +5; the topological surface area was < 150); and the *F*-value of Abbott bioavailability does not exceed 10% (Oldendorf, 1970).

For oral bioavailability and absorption, a drug must have strong aqueous solubility. Based on the latter, three methods, namely Estimated SOLubility (ESOL), A method to compute log S and to estimate the water solubility (ALI) logS, and (SILICOS-IT) logS (Vázquez-Tato *et al*., 2021), are used to estimate the water solubility. The ESOL model is an acronym for calculating aqueous solubility straight from chemical molecular structure, then through molecular weight, the heavy atoms proportion found in the aromatic system, and rotatable bonds number. The model predicted solubility correctly within a factor of 5–8 through three validation sets (Arora *et al*., 2008; Cheng *et al*., 2012). The *in-silico* prediction model of aqueous solubility utilizing logS (ALI) considers the effect of TPSA. By using a fragmental form, Log (SILICOS-IT) calculates the negative sign logarithm of a compound's water solubility. The logS scale ranges from −10 (insoluble), −6 (poorly soluble), −4 (soluble), −2 (extremely soluble), and 0 (highly soluble) (Mishra and Dahima, 2019).

A drug's lipophilic character must be strong enough to allow it to cross the cell membrane and have good biological activity. Several methods can be used to evaluate the lipophilicity parameter. The ilogP (in-house physics-based approach) is based on solvation-free energies using *n*-octanol and water measured using the model of a generalized born and solvent accessible surface area. On the other hand, XlogP3 is an atomistic approach that uses the XlogP software to measure corrective factors and a knowledge-based library. WlogP is a fragmental atomistic process. MlogP is a topological approach that uses 13 molecular descriptors in a linear relationship. a Belgian consultancy company that was founded in 2010 and that is specialized in computational drug design (SILICOS-IT) logP (hybrid method) uses fragment and topological descriptors; logP is a hybrid method. The arithmetic mean of the five lipophilic character predictions is the consensus of logP (Cheng *et al*., 2012).

Figure 2 shows that the radar of bioavailability, revealed by the colored zone, is the best physicochemical space indicator for oral bioavailability when lipophilicity, saturation, size, flexibility, polarity, and solubility are considered. LogP can have lipophilicity of −0.7 to +5.0. The molecular weight can be anywhere between 150 and 500 (g/mol). Between 20 and 130 A^o is the TPSA (Antoine *et al*., 2017). The logS (ESOL) insolubility ranges from 0 to 6. The number of rotatable bonds should range from 0 to 9 and the unsaturation fraction ranges from 0.25 to 1.0, indicating that the carbon atom fraction in sp^3 hybridization cannot be less than 0.25.

According to its physicochemical properties, the compounds' molecular formula is $C_{19}H_{14}FNO_2$. The molecular mass was 307.32 (g/mol). This complex comprises 23 heavy atoms and 12 aromatic heavy atoms. 0.16% of carbon atoms are active in the sp^3 hybridization. There are four rotatable bonds, four hydrogen bond acceptors, and one H-bond donor in this structure. The molar refractivity was found to be 84.70, and the TPSA was measured to be 61.09 A^o (Mishra and Dahima, 2019). The logPo/w (ilogP), logPo/w (XlogP3), logPo/w (WlogP), logPo/w (MlogP), Po/w (SILICOS-IT), and consensus logPo/w were 2.66, 3.64, 3.81, 3.71, 4.91, 3.71, respectively. The logP values mean that the compound is lipophilic in general. With a logS (ESOL) value of −4.05, the compound's water solubility was measured, meaning that it is moderately water-soluble.

The BOILED-egg model was used to study the pharmacokinetic properties. The BOILED-egg model helps in performing the computation of derivative polarity as well as lipophilicity since it generates datasets with high precision, speed, and transparency (Fahmina *et al*., 2020; Sabitu *et al*., 2020). Also, it aids in drug production by allowing chemical libraries to be purified. This model helps for intuitive estimation of passive gastrointestinal absorption (HIA) and brain penetration (BBB) concerning the direction of the molecules (Fig. 3). The yolk (yellow region) represents a high likelihood of brain invasion, while the white area (intestinal tract) represents a high likelihood of passive absorption by the GI tract. It is not appropriate for white and yolk areas to be mutually exclusive.

TUG-770 has a high degree of gastrointestinal absorption and easily passes through the blood–brain barrier. There will be no problems with opioid excretion since there is no P-gp substrate. P-gp is necessary for drug removal and absorption. P-gp has a stronger impact on limiting drug absorption from blood circulation into the brain and from the intestinal lumen into epithelial cells due to its localization than it does on facilitating drug excretion

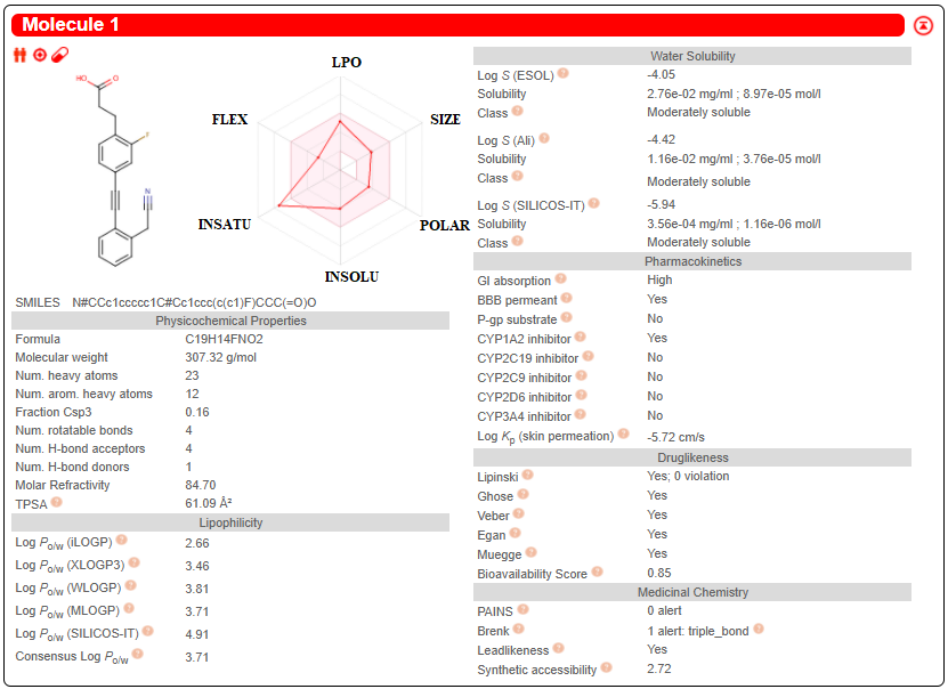

Figure 2. The bioavailability radar of TUG-770 using SwissADME predictor.

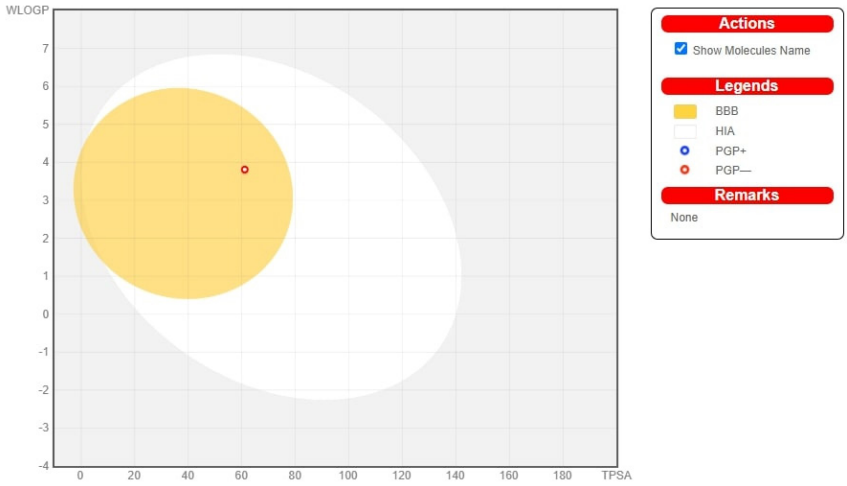

Figure 3. The presence of a molecule in the yolk of an egg indicates that it would be able to cross the blood–brain barrier.

from hepatocytes and renal tubules into the neighboring luminal space due to its localization. Since it activates the isoenzymes CYP2C19 and CYP2D6, there is a risk of aggregation or drug–drug reactions, which could lead to toxicity.

With a bioavailability score of 0.85, the parameter of drug-likeness is considered high, since it fits the Lipinski, Verber, and Egan rule. The score of Synthetic Accessibility of SwissADME is based on the premise that the occurrence of molecular fragments in "really" obtainable molecules is related to synthesis ease. For typical chemical moieties, the fragmental contribution to Synthetic Accessibility should be beneficial, but for uncommon moieties, it should be unfavorable. The synthetic usability score was discovered to be 2.72, suggesting that the molecule is not difficult to synthesize. There is no alarm about Pan-Assay Interference Compounds (PAINS), suggesting that it is a very particular compound.

OUTPUT

We used its incorporation into SwissADME to improve the graphical efficiency by predicting P-gp substrates, which is the most effective active efflux mechanism found in biological barriers. The state of the computation is shown immediately after

Table 1. SwissTargetPrediction.

Target	Common name	Uniprot ID	ChEMBL ID	Target class	Probability*	Known actives (3D/2D)
Free fatty acid receptor 1	FFAR1	O14842	CHEMBL4422	Family A G protein- coupled receptor	1.0	1 74 / 19
G-protein-coupled receptor 120	FFAR4	Q5NUL3	CHEMBL5339	Family A G protein- coupled receptor	1.0	21 / 22
Aldose reductase (by homology)	AKR1B1	P15121	CHEMBL1900	Enzyme	0.101613854776	310 / 0
Matrix metalloproteinase 13	MMP13	P45452	CHEMBL280	Protease	0.101613854776	93 / 0
Matrix metalloproteinase 14	MMP14	P50281	CHEMBL3869	Protease	0.101613854776	23 / 0
Aldo-keto-reductase family 1 member C3	AKR1C3	P42330	CHEMBL4681	Enzyme	0.101613854776	104 / 0
Fatty acid-binding protein, liver (by homology)	FABP1	P07148	CHEMBL5421	Fatty acid binding prote family	in 0.101613854776	3 / 0
Steroid 5-alpha-reductase 2	SRD5A2	P31213	CHEMBL1856	Oxidoreductase	0.101613854776	48 / 0
Matrix metalloproteinase 16	MMP16	P51512	CHEMBL2200	Protease	0.101613854776	3 / 0
Matrix metalloproteinase 8	MMP8	P22894	CHEMBL4588	Protease	0.101613854776	75 / 0
Matrix metalloproteinase 3	MMP3	P08254	CHEMBL283	Protease	0.101613854776	74 / 0
Thyroid hormone receptor alpha	THRA	P10827	CHEMBL1860	Nuclear receptor	0.101613854776	41 / 0
Thyroid hormone receptor beta-1	THRB	P10828	CHEMBL1947	Nuclear receptor	0.101613854776	49 / 0
HMG-CoA reductase	HMGCR	P04035	CHEMBL402	Oxidoreductase	0.101613854776	62 / 0
Thromboxane-A synthase	TBXAS1	P24557	CHEMBL1835	Cytochrome P450	0.101613854776	270 / 0
Mitogen-activated protein kinase kinase kinase 8	MAP3K8	P41279	CHEMBL4899	Kinase	0.101613854776	18 / 0
Plasminogen	PLG	P00747	CHEMBL1801	Protease	0.101613854776	2 / 0
G protein-coupled receptor 44	PTGDR2	Q9Y5Y4	CHEMBL5071	Family A G protein- coupled receptor	0.101613854776	66 / 0
Leukotriene B4 receptor 1	LTB4R	Q15722	CHEMBL3911	Family A G protein- coupled receptor	0.101613854776	41 / 0
Solute carrier family 22 member 12	SLC22A12	Q96S37	CHEMBL6120	Family A G protein- coupled receptor	0.101613854776	1084 / 0
Prostanoid EP4 receptor	PTGER4	P35408	CHEMBL1836			

Target	Common name	Uniprot ID	ChEMBL ID	Target class	Probability*	Known actives (3D/2D)
Angiotensin-converting enzyme (by homology)	ACE	P12821	CHEMBL1808	Protease	0.101613854776	237 / 0
Prostanoid IP receptor	PTGIR	P43119	CHEMBL1995	Family A G protein- coupled receptor	0.101613854776	30 / 0
Thromboxane A2 receptor	TBXA2R	P21731	CHEMBL2069	Family A G protein- coupled receptor	0.101613854776	246 / 0
Hematopoietic cell protein-tyrosine phosphatase 70Z-PEP	PTPN22	Q9Y2R2	CHEMBL2889	Phosphatase	0.101613854776	17 / 0
Peroxisome proliferator-activated receptor delta	PPARD	Q03181	CHEMBL3979	Nuclear receptor	0.101613854776	125 / 0
Carbonic anhydrase II	CA2	P00918	CHEMBL205	Lyase	0.101613854776	94 / 0
Carbonic anhydrase I	CA1	P00915	CHEMBL261	Lyase	0.101613854776	66 / 0
Glutathione reductase	GSR	P00390	CHEMBL2755	Oxidoreductase	0.101613854776	2 / 0
Carbonic anhydrase XII	CA12	O43570	CHEMBL3242	Lyase	0.101613854776	26 / 0
Carbonic anhydrase IX	CA9	Q16790	CHEMBL3594	Lyase	0.101613854776	30 / 0
Cytochrome P450 11B2	CYP11B2	P19099	CHEMBL2722	Cytochrome P450	0.101613854776	1 / 0
Retinoid X receptor alpha	RXRA	P19793	CHEMBL2061	Nuclear receptor	0.101613854776	52 / 0
Phosphodiesterase 5A	PDE5A	O76074	CHEMBL1827	Phosphodiesterase	0.101613854776	5 / 0
Fatty acid binding protein adipocyte	FABP4	P15090	CHEMBL2083	Fatty acid binding protein family	0.101613854776	39 / 0
Phosphodiesterase 3	PDE3A	Q14432	CHEMBL241	Phosphodiesterase	0.101613854776	4 / 0
Phosphodiesterase 7A	PDE7A	Q13946	CHEMBL3012	Phosphodiesterase	0.101613854776	14 / 0
Prostanoid EP2 receptor	PTGER2	P43116	CHEMBL1881	Family A G protein- coupled receptor	0.101613854776	102 / 0
Prostanoid EP3 receptor	PTGER3	P43115	CHEMBL3710	Family A G protein- coupled receptor	0.101613854776	40 / 0
Protein farnesyltransferase	FNTA FNTB	P49354 P49356	CHEMBL2094108	Enzyme	0.101613854776	139 / 6
Matrix metalloproteinase 2	MMP2	P08253	CHEMBL333	Protease	0.101613854776	1084 / 0
Matrix metalloproteinase 12	MMP12	P39900	CHEMBL4393	Protease	0.101613854776	48 / 5
DNA topoisomerase I	TOP1	P11387	CHEMBL1781	Isomerase	0.101613854776	2 / 0
Transitional endoplasmic reticulum ATPase	VCP	P55072	CHEMBL1075145	Primary active transporter	0.101613854776	19 / 0

Target	Common name	Uniprot ID	ChEMBL ID	Target class	Probability*	Known actives (3D/2D)
Peroxisome proliferator-activated receptor gamma	PPARG	P37231	CHEMBL235	Nuclear receptor	0.101613854776	347 / 0
Peroxisome proliferator-activated receptor alpha	PPARA	Q07869	CHEMBL239	Nuclear receptor	0.101613854776	235 / 0
MAP kinase p38 alpha	MAPK14	Q16539	CHEMBL260	Kinase	0.101613854776	45 / 0
Prostanoid DP receptor	PTGDR	Q13258	CHEMBL4427	Family A G protein- coupled receptor	0.101613854776	150 / 0
Interleukin-8	CXCL8	P10145	CHEMBL2157	Secreted protein	0.101613854776	3 / 0
Matrix metalloproteinase 1	MMP1	P03956	CHEMBL332	Protease	0.101613854776	36 / 0
Dihydroorotate dehydrogenase	DHODH	Q02127	CHEMBL1966	Oxidoreductase	0.101613854776	199 / 0
Endothelin receptor ET-A	EDNRA	P25101	CHEMBL252	Family A G protein- coupled receptor	0.101613854776	77 / 0
Phosphodiesterase 4B	PDE4B	Q07343	CHEMBL275	Phosphodiesterase	0.101613854776	105 / 0
Steroid 5-alpha-reductase 1	SRD5A1	P18405	CHEMBL1787	Oxidoreductase	0.101613854776	9 / 0
Androgen Receptor	AR	P10275	CHEMBL1871	Nuclear receptor	0.101613854776	4 / 0
Mineralocorticoid receptor	NR3C2	P08235	CHEMBL1994	Nuclear receptor	0.101613854776	14 / 0
Progesterone receptor	PGR	P06401	CHEMBL208	Nuclear receptor	0.101613854776	16 / 0
Endothelin receptor ET-B	EDNRB	P24530	CHEMBL1785	Family A G protein- coupled receptor	0.101613854776	22 / 0
Aldehyde reductase	AKR1A1	P14550	CHEMBL2246	Enzyme	0.101613854776	18 / 0
Protein-tyrosine phosphatase 1B	PTPN1	P18031	CHEMBL335	Phosphatase	0.101613854776	93 / 0
Lysophosphatidic acid receptor Edg-4	LPAR2	Q9HBW0	CHEMBL3724	Family A G protein- coupled receptor	0.101613854776	9 / 0
Aldo-keto reductase family 1 member B10	AKR1B10	O60218	CHEMBL5983	Enzyme	0.101613854776	14 / 0
Heat shock protein HSP 90-alpha	HSP90AA1	P07900	CHEMBL3880	Other cytosolic protein	0.101613854776	19 / 0
Fatty acid binding protein intestinal	FABP2	P12104	CHEMBL4879	Fatty acid binding protein family	0.101613854776	2 / 0
Lysine-specific demethylase 2A	KDM2A	Q9Y2K7	CHEMBL1938210	Eraser	0.101613854776	22 / 0
Lysine-specific demethylase 5C	KDM5C	P41229	CHEMBL2163176	Eraser	0.101613854776	25 / 0
Muscarinic acetylcholine receptor M1	CHRM1	P11229	CHEMBL216	Family A G protein- coupled receptor	0.101613854776	7 / 0
Transforming protein RhoA	RHOA	P61586	CHEMBL6052	Unclassified protein	0.101613854776	5 / 0

Target	Common name	Uniprot ID	ChEMBL ID	Target class	Probability*	Known actives (3D/2D)
Monocarboxylate transporter 4	SLC16A3	O15427	CHEMBL2073663	Electrochemical transporter	0.101613854776	4 / 0
Peptidyl-glycine alpha-amidating monooxygenase	PAM	P19021	CHEMBL2544	Enzyme	0.101613854776	3 / 0
Peptidyl-prolyl cis-trans isomerase NIMA- interacting 1	PIN1	Q13526	CHEMBL2288	Enzyme	0.101613854776	41 / 0
Epoxide hydratase	EPHX2	P34913	CHEMBL2409	Protease	0.101613854776	53 / 0
Telomerase reverse transcriptase	TERT	O14746	CHEMBL2916	Enzyme	0.101613854776	2 / 0
Nuclear receptor ROR-gamma	RORC	P51449	CHEMBL1741186	Nuclear receptor	0.101613854776	9 / 0
Hepatocyte growth factor receptor	MET	P08581	CHEMBL3717	Kinase	0.101613854776	5 / 0
Serine/threonine-protein kinase Aurora-A	AURKA	O14965	CHEMBL4722	Kinase	0.101613854776	49 / 0
Histone deacetylase 3	HDAC3	O15379	CHEMBL1829	Eraser	0.101613854776	1 / 0
Histone deacetylase 6	HDAC6	Q9UBN7	CHEMBL1865	Eraser	0.101613854776	2 / 0
Xanthine dehydrogenase	XDH	P47989	CHEMBL1929	Oxidoreductase	0.101613854776	1 / 0
Histone deacetylase 2	HDAC2	Q92769	CHEMBL1937	Eraser	0.101613854776	1 / 0
Methionyl-tRNA synthetase	MARS	P56192	CHEMBL2870	Enzyme	0.101613854776	15 / 0
Histone deacetylase 8	HDAC8	Q9BY41	CHEMBL3192	Eraser	0.101613854776	1 / 0
Histone deacetylase 1	HDAC1	Q13547	CHEMBL325	Eraser	0.101613854776	1 / 0
Histone deacetylase 10	HDAC10	Q969S8	CHEMBL5103	Eraser	0.101613854776	1 / 0
Phosphodiesterase 4D	PDE4D	Q08499	CHEMBL288	Phosphodiesterase	0.101613854776	74 / 0
Casein kinase II alpha	CSNK2A1	P68400	CHEMBL3629	Kinase	0.101613854776	128 / 0
Autotaxin	ENPP2	Q13822	CHEMBL3691	Enzyme	0.101613854776	28 / 0
Lysosomal protective protein	CTSA	P10619	CHEMBL6115	Protease	0.101613854776	311 / 0
Neprilysin (by homology)	MME	P08473	CHEMBL1944	Protease	0.101613854776	189 / 0
Phospholipase A2 group IIA	PLA2G2A	P14555	CHEMBL3474	Enzyme	0.101613854776	80 / 0
P2X purinoceptor 7	P2RX7	Q99572	CHEMBL4805	Ligand-gated ion channel	0.101613854776	1 / 0
Arachidonate 5-lipoxygenase	ALOX5	P09917	CHEMBL215	Oxidoreductase	0.101613854776	83 / 0
Lysine-specific demethylase 5A	KDM5A	P29375	CHEMBL2424504	Eraser	0.101613854776	7 / 0
Lysine-specific demethylase 5B	KDM5B	Q9UGL1	CHEMBL3774295	Eraser	0.101613854776	5 / 0
Lysine-specific demethylase 2B	KDM2B	Q8NHM5	CHEMBL3779760	Eraser	0.101613854776	3 / 0
MAP kinase ERK2	MAPK1	P28482	CHEMBL4040	Kinase	0.101613854776	7 / 0
Hydroxyacid oxidase 1	HAO1	Q9UJM8	CHEMBL4229	Enzyme	0.101613854776	9 / 0
Apoptosis regulator Bcl-X	BCL2L1	Q07817	CHEMBL4625	Other ion channel	0.101613854776	29 / 0
G protein-coupled receptor kinase 6	GRK6	P43250	CHEMBL6144	Kinase	0.101613854776	16 / 0
Lysine-specific demethylase 4C	KDM4C	Q9H3R0	CHEMBL6175	Eraser	0.101613854776	18 / 0

*Probability for the query molecule-assumed as bioactive – to have this protein as target.

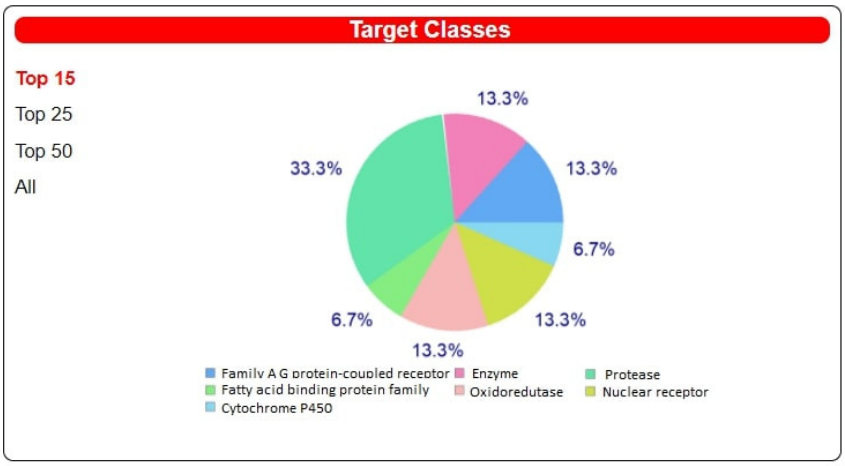

Figure 4. Page showing the outcome of the prediction. The projected targets for the question molecule are shown on this page. Like their scores, targets are ranked. The distribution of goal groups is shown in a pie chart which is used to denote predictions dependent on homology.

application, beginning with validation of structure. This transient page communicates with the workload management system (Slurm version 17.11.2) to inform the user that his or her job has been queued or is being worked on. The consumer will see the various stages of the computation and observe the overall procedure on a progress bar. Starting calculations take between 15 and 20 seconds for a compound the size of a druglike molecule. Predictions are shown on the first performance page until the progression bar is filled (Antoine *et al*., 2017).

The most valuable piece of information on this result page is the tabulated list of potential protein targets (Table 1), as determined by the dual-score ligand-dependent reverse screening of the query molecule against the collection of known actives. The table rows are ranked by default based on the likelihood of the related protein being the real target of the query molecule. Protein complex targets are now provided incomplete names (linked to a particular ChEMBL ID), with their subunits/components linked to Genecard and Uniprot separately in version 2019.

The probability values, shown as green bars, are calculated using the combined scores of the most closely related compounds to the query molecule (in 2D and 3D) that are active on a given protein as previously stated, and outlined in detail elsewhere (Antoine *et al*., 2019; Gfeller *et al*., 2014). Importantly, this value accurately depicts the likelihood of a bioactive molecule having a specific protein as a goal, but not the likelihood of being bioactive. Furthermore, targets labeled with the phrase "by homology" are projections focused on related molecules active on proteins with a high degree of homology (Antoine *et al*., 2017).

A common example is an orthology in which a target is expected for a given species depending on the question molecule's similarities to compounds active on ortholog proteins. In the last column, you can see the number of compounds that are active on each listed target and are extremely like the query molecule. You may adjust the number of planned targets shown on a website to 15 (default), 25, 50, or all using page scanning (maximum 100). Furthermore, by clicking on the header, the table can be arranged by any column, and the results can be filtered using a search box. Furthermore, users can use advanced export options by clicking on dedicated icons. The table can be saved in a variety of formats such as CSV, Excel, and PDF, copied or printed straight from the browser. A pie chart created with JPgraph is shown in a box located on the top-right of the result sheet (Fig. 4) as a description of the forecast target groups (column 5 of Table 1) (version 4.2.6). The percentages equate to the top 15 proteins by design, but the user can change this by selecting the top 25, 50, or all expected targets using the buttons on the left of the column. By clicking on the pie-chart, a full-size image would appear in a new tab of the window, allowing for more saving or printing. The user's question molecule's chemical composition is shown in a box located on the top-left side of the result sheet (Fig. 4). the molecular modeling group of the SIB Swiss Institute of Bioinformatics has created four icons that appear within this box and allow for the clear submission of the molecule of interest to other web resources provided. These interoperability symbols can be used in all boxes referring to the chemical compositions of known actives, as well as a reference to the ChEMBL Compound Report Card.

The above is classified in order of their similarity to the question molecules, from most to least. The "twins" icon sends the molecule to SwissSimilarity for ligand-based direct screening (Daina and Zoete, 2017), the "target" icon resubmits the aim prediction (on a different animal, for example), and the "pill" icon uses SwissADME to approximate physicochemical, ADME, or pharmacokinetic parameters (Zoete *et al*., 2016). The proposed expansion of interoperability by adding other in-house software is also in the works, so more icons will be added to the various websites in the future (Antoine *et al*., 2017). Obtaining the molecule's SMILES through the fourth symbol also makes it easier to use it as a possible input to other, potentially external, processes. The ChEMBL ID, SMILES, similarity attribute to the query molecule, and, if applicable, the source species of the experimentally identified homologous target are all included in the file (Antoine *et al*., 2017).

Figure 4 shows a brief of the various target groups present among the projected targets in a pie chart. The chance calculated

from the goal scores is shown as a horizontal bar in the fifth column. Ligands are sorted by how close they are to the question molecule. The ligands have a relation to their ChEMBL entries, and the resemblance to the question molecule is suggested. We propose that you explore the ligands manually that are closest and the query molecule to see how accurate the projections are, and which types of ligands have the most similarities to the query molecule. Finally, there are support pages along with interactive screenshots of the website, a FAQ page to help users, and a download page to get a little of the raw data used in the predictions process.

CONCLUSION

Traditional clinical trial methods require a significant expenditure in time and resources, and it is possible that the molecule will fail. Thus, to minimize or change the structure, *in silico* trials can be pursued rather than aggressively pursuing monopoly and running to animal studies. The SwissADME web tool allows users to calculate vital pharmacokinetic, physicochemical, and similar parameters for one or more molecules. It was inferred from the analysis that the compound's aqueous solubility, as well as the sp^3 hybridized carbon atoms fraction, should be increased. Further changes to the lead structure are needed to guarantee that the molecule does not hinder metabolizing enzymes.

SwissTargetPrediction is considered part of the Swiss Institute of Bioinformatics' valuable initiative to offer online resources for computer-assisted drug design. SwissTargetPrediction can be combined further with these methods in the future, for example, by forecasting possible linking modes with Swiss-Dock (Gabriela and Walter, 2019; Gfeller *et al*., 2014).

TUG-770 has a high degree gastrointestinal absorption rate and quickly passes the blood-brain barrier. Because there is no P-gp substrate, there will be no issues with opioid excretion. Also, with its bioavailability score of 0.85, the drug-likeness parameter is considered high, since it meets the Lipinski, Verber, and Egan rules. Additionally, TUG-770 synthetic usability score was determined to be 2.72, indicating that the molecule is not difficult to synthesis. Moreover, the logP values indicate that the compound is lipophilic in general. The compound's water solubility was determined with a logS (ESOL) value of −4.05, indicating that it is moderately water-soluble.

ACKNOWLEDGMENT

Declared None declared.

FUNDING

There is no funding to report.

CONFLICTS OF INTEREST

The authors report no financial or any other conflicts of interest in this work.

ETHICAL APPROVALS

This study does not involve experiments on animals or human subjects.

DATA AVAILABILITY

All data generated and analyzed are included within this research article.

PUBLISHER'S NOTE

This journal remains neutral with regard to jurisdictional claims in published institutional affiliation.

AUTHORS' CONTRIBUTIONS

All authors made significant contributions to the conception and design, acquisition of data, and analysis and interpretation of data. Also, they took part in writing the draft of the article and revising it in a better way; and agreed to submit to the current journal. They agreed about the final approval of the version to be published; and agreed to be accountable for all aspects of the work.

REFERENCES

Akbar A, Mohamed EIB, Raza S, Wajid R, Yeldez ELK, El Sayed ElAS, Nawaz T. Synthesis, characterization and *in-silico* ADMET screening of mono- and dicarbmethoxylated 6,6'-methylenebis(2-cyclohexyl-4-methylphenol) and their hydrazides and hydrazones. Der Chem Sin, 2017; 8:446−60.

Antoine D, Olivier M, Vincent Z. SwissADME: a free web tool to evaluate pharmacokinetics, druglikeness and medicinal chemistry friendliness of small molecules. Sci Rep, 2017; 7:1−13.

Antoine D, Olivier M, Vincent Z. SwissTargetPrediction: updated data and new features for efficient prediction of protein targets of small molecules. Nucleic Acids Res, 2019; 47:W357–64.

Arora T, Mehta AM, Sharma KK. Substitute of animals in drug research: an approach towards fulfillment of 4R's. Indian J Pharm Sci, 2008; 73:1−6.

Cheng F, Li W, Zhou Y, Shen J, Wu Z, Liu G, Lee PW, Tang Y. admetSAR: a comprehensive source and free tool for assessment of chemical ADMET properties. J Chem Info Model, 2012; 52:3099−105.

Daina A, Michielin O, Zoete V. iLOGP: a simple, robust and efficient description of *n*-octanol/water partition coefficient for drug design using the GB/SA approach. J Chem Info Model, 2014; 54:3284−301.

Daina A, Zoete V. A BOILED-Egg to predict gastrointestinal absorption and brain penetration of small molecules. Chem Med Chem, 2016; 11:1117–21.

Daina A, Zoete V. SwissADME: a free web tool to evaluate pharmacokinetics, drug likeness and medicinal chemistry friendliness of small molecules. Sci Rep, 2017; 7:1−13.

Fahmina Z, Anjali G, Karthick T, Kavita K, Ali AS, Anujit G, Poonam T, Nahid N. Physicochemical and pharmacokinetic analysis of anacardic acid derivatives. ACS Omega, 2020; 5:6021−30.

Gabriela BF, Walter FAJ. Docking with SwissDock. Meth Mol Biol, 2019; 2053:189−202.

Gfeller D, Grosdidier A, Wirth M, Daina A, Michielin O, Zoete V. SwissTargetPrediction: a web server for target prediction of bioactive small molecules. Nucleic Acids Res, 2014; 42:W32–8.

Guoli X, Zhenxing W, Jiacai Y, Li F, Zhijiang Y, Changyu H, Mingzhu Y, Xiangxiang Z, Chengkun W, Aiping L, Xiang C, Tingjun H, Dongsheng C. ADMETlab 2.0: an integrated online platform for accurate and comprehensive predictions of ADMET properties. Nucleic Acids Res, 2021; 49:W5–14.

Kaitin KI. Obstacles and opportunities in new drug development. Clin Pharmacol Ther, 2008; 83:210−2.

Leonardo LGF, Adriano DA. ADMET modeling approaches in drug discovery. Drug Discov, 2019; 24:1157−65.

Longfei G, Hongbin Y, Yingchun C, Lixia S, Peiwen D, Weihua L, Guixia L, Yun T. ADMET-score—a comprehensive scoring function for evaluation of chemical drug-likeness. Medchemcomm, 2019; 10:148–57.

Mishra S, Dahima R. *In-vitro* ADME studies of TUG-891, a GPR-120 inhibitor using SwissADME predictor. J Drug Deliv Ther, 2019; 9:266−369.

Noemi ADI, Bárbara IDE, José LMF. *In silico* ADME/Tox profiling of natural products: a focus on BIOFACQUIM. ACS Omega, 2020; 5:16076–84.

Oldendorf WH. Measurement of brain uptake of radiolabeled substances using a tritiated water internal standard. Brain Res, 1970; 24:372−6.

Pires DEV, Blundell TL, Ascher DB. pkCSM: predicting small-molecule pharmacokinetic and toxicity properties using graph-based signatures. J Med Chem, 2018; 58:4066−72.

Potts RO, Guy RH. Predicting skin permeability. Pharm Res, 1992; 9:663–9.

Sabitu BO, Adamu U, Gideon S, Sani U. QSAR modeling, molecular docking and ADMET/pharmacokinetic studies: a chemometrics approach to search for novel inhibitors of norepinephrine transporter as potent antipsychotic drugs. J Iran Chem Soc, 2020; 17:1953–66.

Tianshu Y, Yunkai Y, Yan W. Predictive biomarkers and potential drug combinations of epi-drugs in cancer therapy. Clin Epigenetics, 2021; 13:113−31.

Vázquez-Tato MP, Julio AS, Francisco M, Francisco F, Santiago de F, Javier M, Juan VT, Aida J, Victor HS, José VT. Highly hydrophilic and lipophilic derivatives of bile salts. Int J Mol Sci, 2021; 22:6684−98.

Yuhua L, Qiang M, Mengbi Y, Dongyang L, Xiangyu H, Lan T, Xin W, Yuanfeng L, Xiaoyan C, Kexin L, Ai-Ming Y, Zhong Z, Huichang B. Current trends in drug metabolism and pharmacokinetics. Acta Pharm Sin B, 2019; 6:1113−44.

Yusuf I, Adamu U, Sani U. Computational studies of a series of 2-substituted phenyl-2-oxo-, 2-hydrox-yl- and 2-acylloxyethylsulfonamides as potent anti-fungal agents. Heliyon, 2020; 6:1−6.

Zoete V, Daina A, Bovigny C, Michielin O. SwissSimilarity: a web tool for low to ultra-high throughput ligand-based virtual screening. J Chem Inform Comput Sci, 2016; 56:1399–404.

How to cite this article:
Al Azzam KM, Negim ES, Aboul-Enein HY. ADME studies of TUG-770 (a GPR-40 inhibitor agonist) for the treatment of type 2 diabetes using SwissADME predictor: *In silico* study. J Appl Pharm Sci, 2022; 12(04):159–169.